Improved push-pull-push *E*-Bodipy fluorophores for two-photon cell-imaging

Pascal Didier,[a] Gilles Ulrich,[b] Yves Mély[a] and Raymond Ziessel*[b]

Received 12th June 2009, Accepted 9th July 2009
First published as an Advance Article on the web 23rd July 2009
DOI: 10.1039/b911587k

Quadrupolar Bodipy dyes exhibiting TPA activity and high brightness with an emission at 660 nm were synthesized and internalized in HeLa cells, whereupon FLIM experiments were conducted.

Optical imaging is one of the most attractive techniques commonly used in biomedical research.[1] Recent progress has raised new demands for dyes with improved properties including good solubility, biocompatibility, chemo- and photo-stability, one and two photon excitation, high brightness when internalized into cells, and minimal cytotoxicity.[2] Internalization in cells can be realized by using a vector that facilitates cell entry and may promote selective localization in a given organelle.[3] Alternatively, the chemical structure of the dye can be modified to favour cell penetration.[4] We recently developed a new class of diethynyl dipyrromethene-boron dyes (*E*-Bodipy) that can be modified at will, and present improved stability without detriment to the optical properties.[5] To extend the development of stable dyes emitting in the 600 to 800 nm range, a window widely recognized as being attractive for bioanalysis and *in vivo* imaging,[6] we have now developed new dyes emitting around 660 nm as well as being stable (ethynyl substitution at the boron), cell permeable, and having a pronounced internal quadrupole (push-pull-push), a prerequisite for two photon absorption spectroscopy and imaging.[7] We report here the design, the one- and two-photon photophysical properties and the two-photon imaging applications of these improved *E*-Bodipy fluorophores.

The target dyes **1** and **2** were prepared in two steps according to Scheme 1: (i) a Knoevenagel condensation of the 3,5-methyl groups with 4-methoxybenzaldehyde in basic conditions[8] to provide the styryl derivatives; (ii) boron substitution using the appropriate Grignard reagents to afford the novel dyes in good yields.[9] The use of short methoxyethyleneglycol was inspired by the previous use of PEG (PEG-PE or PEG-DSPE) for drug vectors[10] or Bodipy[4] cell internalization and phototherapy. Single photon excitation around 647 nm resulted in strong emission in the red (662 nm). The brightness, expressed as $\phi_{fluo}\varepsilon$ was found to lie at 90 750 for **1** and 67 900 for **2** (Table 1). The redox behaviour in solution was consistent with reversible radical anion and radical cation formation and successive irreversible styryl oxidation (Table 2).[11] Little redox quenching is expected in standard biological conditions keeping in mind the modest oxidation potentials of dyes **1** and **2** in the excited state (E_0 $B^*/B^{-\bullet} \approx 0.82$ V *vs* SCE, $E_{00} = 1.95$ eV) and the weak reducing environment of a living cell.[12] As expected from the design of the dyes, the presence of a strong electron donor (styrylanisole push moieties) and the electron accepting abilities of the Bodipy (pull moieties) resulted in a pronounced intramolecular charge transfer (ICT) observed at 370 nm in both dyes (Fig. 1). This type of transition greatly enhances the two photon absorption cross-section (TPACS).[13]

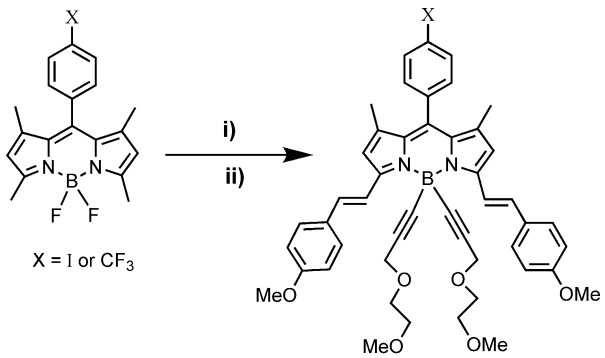

Scheme 1

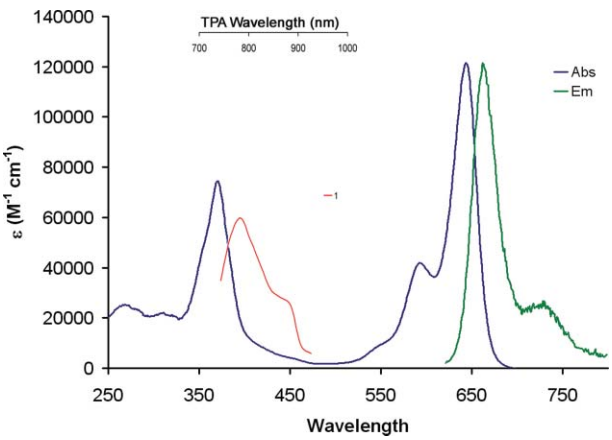

Fig. 1 Absorption (blue) and emission (green) spectra for compound **1** in CH_2Cl_2 at rt. TPA action cross section (GM) for **1** (red). The excitation power was 1 mW at the sample level and was kept constant for all wavelengths.

The absolute two-photon absorption (TPA) action cross section ($\phi\delta$) was determined using interferometric autocorrelations and eqn (1):[15]

$$\phi\delta = \frac{f\left[\int_{-T}^{T} F(\tau) - 2TF_{\infty}\right]}{2c\eta\frac{8n}{\pi\lambda}\langle P_0(t)\rangle^2} \quad (1)$$

[a]*Laboratoire de Chimie Organique et Spectroscopie Avancées (UMR7515-CNRS), École de Chimie, Polymères, Matériaux (ECPM), 25 rue Becquerel, 67087 Strasbourg Cedex, France*
[b]*Laboratoire de Biophotonique et Pharmacologie, UMR 7213 CNRS, Université de Strasbourg, Faculté de Pharmacie, 74 route du Rhin, 67401 ILLKIRCH Cedex, France*

Table 1 Spectroscopic data in dichloromethane solution at 298 K

Compds	λ_{abs} (nm)	ε ($M^{-1}cm^{-1}$)	λ_F (nm)	Φ_F[a]	$\varepsilon \times \Phi_F$	τ_F (ns)	k_r[b] (10^8 s^{-1})	k_{nr}[b] (10^8 s^{-1})	ΔG_{ES}[c] eV	E° $B^*/B^{-\bullet}$ eV[d]
1	643	121 000	663	0.75	90 750	5.6	1.34	0.45	1.95	+0.82
2	646	97 000	662	0.70	67 900	6.7	1.04	0.45	1.95	+0.87

[a] At a concentration of 5×10^{-7} M using cresyl violet as a reference $\Phi = 0.51$ in ethanol, $\lambda_{exc} = 578$ nm.[14] All Φ_F are corrected for changes in refractive index. [b] Calculated using the following equations: $k_r = \Phi_F/\tau_F$, $k_{nr} = (1 - \Phi_F)/\tau_F$, assuming that the emitting state is produced with unit quantum efficiency. [c] Excited state energies were estimated (± 5%) by drawing a tangent on the high energy side of the emission. [d] Calculated excited state oxidation potential *vs* SCE, E° $(B^*/B^{-\bullet}) = E^\circ$ $(B/B^{-\bullet}) + \Delta G_{ES}$. B accounts for Bodipy.

Table 2 Electrochemical data for the BODIPY dyes[a]

Cmpds	E°′(ox, soln) (V), ΔE (mV)	E°′(red, soln) (V), ΔE (mV)	HOMO–LUMO gap (eV)
1	+0.67 (60), + 1.09 (irrv.),* + 1.25 (irrv.)**	−1.13 (60) −1.97 (irrv.)	1.80
2	+0.69 (70), + 1.10 (irrv.),* + 1.25 (irrv.)**	−1.08 (70) −1.88 (irrv.)	1.77

[a] Potentials determined by cyclic voltammetry in deoxygenated dichloromethane solution, containing 0.1 M $TBAPF_6$, [electrochemical window from +1.6 to −2.2 V], at a solute concentration of *ca.* 1.5 mM and at rt. Potentials were standardized *versus* ferrocene (Fc) as internal reference and converted to the SCE scale assuming that $E_{1/2}$ $(Fc/Fc^+) = +0.38$ V ($\Delta Ep = 60$ mV) *vs* SCE. Error in half-wave potentials is ±10 mV. For irreversible processes the peak potentials (E_{ap} or E_{cp}) are quoted. All reversible redox steps result from one-electron processes. * Irreversible oxidation of one styryl unit and ** Irreversible oxidation of the second styryl unit.

where ϕ is the quantum yield of the chromophore, δ is the TPA action cross section, f the repetition rate of the laser, T the total acquisition time window, F_∞ is the fluorescence signal for infinite delay, η the detection efficiency of the experimental set-up, c the concentration of the chromophore, n the refractive index of the solvent, λ the laser wavelength and $P_0(t)$ the average incident power on the sample. The TPA action spectra are given in Fig. 2 for dyes **1** and **2** in DMSO, as a function of the laser wavelength. Tetramethylrhodamine (TMR) was used as a reference compound (Fig. 2). The two novel dyes have high TPA action cross sections (72 and 60 GM respectively for **1** and **2**) around 780 nm, approximately twice the wavelength of the linear absorption of the S_0–S_2 transition band of the chromophores (Fig. 1). This two-photon transition takes place from the ground state S_0 to the lowest excited state with similar geometry, being S_2 in this centrosymmetric system.[16] Note that both dyes exhibit a two fold enhancement of the TPA action cross section compared to TMR in water (Fig. 2).

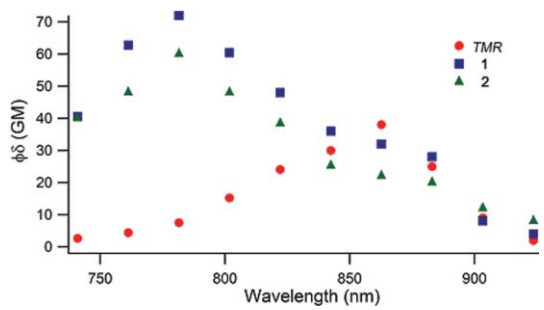

Fig. 2 Two-photon absorption action cross section spectra of TMR (water), compounds **1** and **2** (DMSO) determined by interferometric autocorrelations.

To further characterize the non-linear optical properties of the compounds, fluorescence correlation spectroscopy (FCS) measurements were carried out to characterize the translational dynamics of the dyes.[17] By using the intensity fluctuations of the fluorescent species within a femtoliter volume (defined by the laser excitation), several physical parameters such as the diffusion time, local concentration and the molecular brightness, which are related to the hydrodynamic and photophysical properties, can be monitored. The molecular brightness (*i.e.* the number of photons emitted by a particle per second for a given excitation intensity) of **1** and **2** in DMSO ($\lambda_{exc} = 780$ nm) was compared to the molecular brightness of TMR in water ($\lambda_{exc} = 860$ nm), as a function of the laser power at the sample level (Fig. 3).

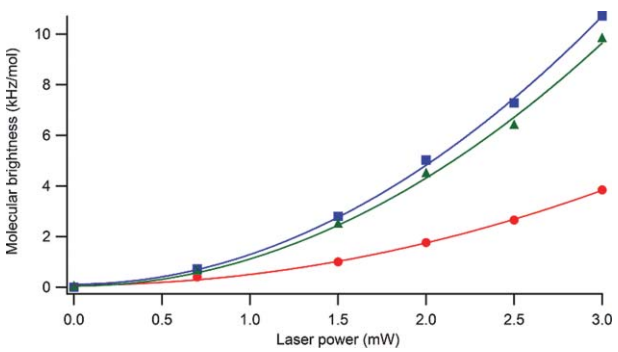

Fig. 3 Molecular brightness measured by FCS as a function of laser power at the sample level for **1** (blue) and **2** (green) in DMSO ($\lambda_{exc} = 780$ nm) and TMR (red) in water ($\lambda_{exc} = 860$ nm). The solid lines correspond to a second order polynomial fit ($y = aP^2$).

As expected from the TPA measurements, the molecular brightness displayed a quadratic dependence with respect to the applied laser power. The molecular brightness of **1** and **2** showed a strong increase compared to that of TMR, which is auspicious for use in two-photon excitation microscopy. Indeed, in non-linear microscopy the molecular brightness of the fluorescent dye is generally a limiting factor for cellular imaging.

To demonstrate the possible utility of the newly synthesized chromophores for two-photon excitation microscopy, fluorescence

lifetime imaging microscopy (FLIM) experiments were performed on Hela cells incubated for 6 h in an aqueous solution with 0.2% of DMSO containing the dyes. The cells were then washed several times with a buffer (PBS) solution and imaged under two-photon excitation. The FLIM images obtained for **1** and **2** are reported in Fig. 4a and b respectively.

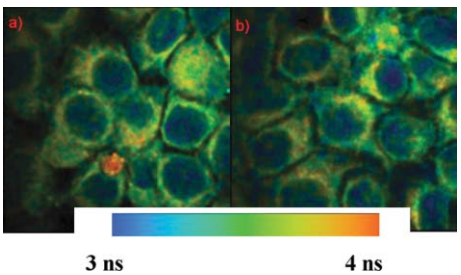

Fig. 4 HeLa cells were incubated for 6 h in a aqueous solution with 0.2% of DMSO containing the dyes. FLIM images for **1** (a) and **2** (b) were obtained with a 2 mW excitation power at the sample level. The corresponding lifetime colour scale is given at the bottom.

From these experiments, many interesting features were established: (i) these novel dyes can be efficiently internalized within the living cells; (ii) no change in the cell morphology is induced by incubating the dyes for at least 3 h, suggesting the absence of significant cytotoxicity; (iii) the lifetime distribution over the cells is not homogeneous and likely due to the aggregation of the dye, as confirmed by brightness analysis in FCS experiments within the cells. The lifetime decrease in the nucleus could be due to a higher aggregation rate in proximity to DNA and a probable electron transfer to nucleic bases such as guanine.[18] We have previously shown that aggregation of Bodipy in DNA results in complete extinction of the fluorescence in the major groove of the polynucleotide.[19]

Due to the relative ease of synthesis of these *E*-Bodipy dyes, their relatively high emission quantum yield and brightness in the red spectral region (70–75%), their improved TPA action cross section compared to TMR and their lack of cytotoxicity, they represent promising candidates for imaging application and diagnostic tools. The good results obtained with these model compounds prompted us to investigate the preparation of efficient water-soluble TPA active Bodipy dyes, able to be bioconjugated. This research is currently in progress.

Experimental

Materials and methods

Chromatographic purification was conducted using 40–63 μm silica gel. Thin layer chromatography (TLC) was performed on silica gel plates coated with fluorescent indicator.

Spectroscopic measurements

300 and 400 (^{1}H), 75.47 (^{13}C) MHz NMR spectra were recorded at room temperature using perdeuterated solvents with residual protiated solvent signals providing internal references. UV–is spectra were recorded using a Shimadzu UV-3600 dual-beam grating spectrophotometer with a 1 cm quartz cell. Fluorescence spectra were recorded on a HORIBA Jobin-Yvon Fluoromax 4P spectrofluorimeter. All fluorescence spectra were corrected. The fluorescence quantum yield (ϕ_{exp}) was calculated from eqn (2). Here, F denotes the integral of the corrected fluorescence spectrum, A is the absorbance at the excitation wavelength, and n is the refractive index of the medium. The reference systems used were rhodamine 6G in methanol ($\phi_{ref} = 0.78$, $\lambda_{exc} = 488$ nm) and cresyl violet in ethanol ($\phi_{ref} = 0.50$, $\lambda_{exc} = 546$ nm)[14] in air-equilibrated water and de-aerated solutions.

$$\Phi_{\exp} = \Phi_{ref}\frac{F\{1-\exp(-A_{ref}\ln 10)\}n^2}{F_{ref}\{1-\exp(-A\ln 10)\}n_{ref}^2} \quad (2)$$

Luminescence lifetimes were measured on a PTI QuantaMaster spectrofluorimeter, using TimeMaster software with Time-Correlated Single Photon Mode coupled to a stroboscopic system. The excitation source was a thyratron-gated flash-lamp filled with nitrogen gas. No filter was used for the excitation. An interference filter centred at 550 nm selected the emission wavelengths. The instrument response function was determined by using a light-scattering solution (LUDOX).

The two-photon absorption cross section (TPACS) measurements were performed on a home-made system. Briefly, the set-up is based on a modified widefield epi-fluorescence microscope (IX70, Olympus, Japan) with an Olympus 40× 0.9NA air objective. Two-photon excitation (TPE) was provided by a titanium:sapphire laser (Tsunami Spectra-Physics). To perform absolute TPACS measurements between 740 and 920 nm, a Michelson interferometer was incorporated in the optical path between the laser and the microscope. By applying a slowly varying voltage with a frequency generator on one arm of the interferometer, an interference pattern is generated in the focal plane of the microscope. Photon detection was performed with an Avalanche Photodiode (SPCM-AQR-14-FC, Perkin Elmer) connected to a time-correlated single photon counting (TCSPC) module (SPC830, Becker & Hickl, Germany) running in the FIFO mode. In the TPE regime, the solution of fluorescent molecules acts as a non-linear medium that allows the measurement of an interferometric autocorrelation from which it is possible to deduce the absolute TPACS of the dyes.

FCS measurements were performed on a home-built two-photon system set-up.[20,21] Photons were detected with an Avalanche Photodiode (APD SPCM-AQR-14-FC, Perkin Elmer) and the normalized autocorrelation function was calculated on-line with a hardware correlator (ALV5000, ALV GmbH). FCS measurements were sequentially repeated, typically 20 × 30 s with an excitation power around 3 mW at the sample level. Each FCS curve was then fitted independently with the standard 3D diffusion model $G(t)=(1/N)*(1 + t/t_D)^{-1}*(1 + t/(S^2t_D)^{-1/2}$, where N is the average number of fluorescent species in the focal volume, t the lag time, t_D the average residence time in the focal volume and S is the ratio between the equatorial and axial radii of the focal volume. The experimental curves were analysed with an Igor Pro (Wavemetrics) function written to automatically process the data. The molecular brightness of the fluorescent species diffusing through the excitation volume was obtained by dividing the average fluorescence intensity <F> by N.

Time-correlated single-photon counting FLIM was performed using a home-made multi-photon laser scanning microscope sharing the same core as the system described for TPACS measurements.[22] For FLIM, a 60X 1.2NA water immersion objective was used and the laser power was adjusted to give count

rates with peaks up to as few as 10^6 photons s^{-1}, so that the pile-up effect can be neglected. Imaging was carried out with a laser scanning system using two fast galvo mirrors (Model 6210, Cambridge Technology), operating in the descanned fluorescence collection mode. The fluorescence was directed to a fiber coupled APD (SPCM-AQR-14-FC, Perkin Elmer), which was connected to a time-correlated single photon counting (TCSPC) module (SPC830, Becker & Hickl), operated in the reversed start-stop mode. Typically, the samples were scanned continuously for about 30 s to achieve appropriate photon statistics to analyse the fluorescence decays. Data were analysed using a commercial software package (SPCImage V2.9, Becker & Hickl, Germany), which uses an iterative reconvolution method to recover the lifetimes from the fluorescence decays.

Chemicals. Ethylmagnesium bromide (1 M solution in THF), *p*-methoxybenzaldehyde were purchased from Aldrich and used as received without further purification. 8-(4-Iodophenyl)-1,3,5,7-tetramethyl-4,4-difluoro-4-bora-3a,4a-diaza-s-indacene[23] was synthesized as previously described. 8-(4-Trifluoromethylphenyl)-1,3,5,7-tetramethyl-4,4-difluoro-4-bora-3a,4a-diaza-s-indacene was synthesized following the same procedure starting from 4-trifluoromethylbenzoyl chloride.

8-(4-Iodophenyl)-1,7-dimethyl-3,5-bis(4-methoxy-styryl-)-4,4-bis(2,5-dioxaoct-7-ynyl)-4-bora-3a,4a-diaza-s-indacene (1). To a solution of 2,5-dioxaoct-7-yne (0.084 g, 0.728 mmol) in anhydrous THF (5mL), at room temperature, was added ethylmagnesium bromide (1.0 M in THF, 0.65 ml). This mixture was stirred 2 h at 60 °C, then this solution was transferred to a Schlenk tube containing 8-(4-iodophenyl)-1,7-dimethyl-3,5-bis(4-methoxy-styryl-)-4,4-difluoro-4-bora-3a,4a-diaza-s-indacene (obtained by a standard procedure)[8] (70 mg, 0.146 mmol) in anhydrous THF (5mL). The mixture was then stirred at 60 °C for 12 h. After addition of water, the organic fraction was extracted with dichloromethane. After removal of the organic solvent, chromatography (silica, dichloromethane/ethyl acetate, gradient from 99:1 to 95:5), afforded compound **1** as purple–greenish powder (70 mg, 55%). ^{1}H NMR ($CDCl_3$, 300 MHz): δ = 1.47 (s, 6H), 3.14–3.16 (m, 4H), 3.19 (s, 6H), 3.50–3.53 (m, 4H), 3.86 (s, 6H), 4.16 (s, 4H), 6.63 (s, 2H),7.10–7.16 (m, 4H), 7.28 (ABsys, 8H, JAB = 8.6 Hz, ν0δ = 188.3 Hz), 7.84 (d, 2H, J = 8.1 Hz), 8.10 (d, 2H, J = 16.4 Hz); ^{13}C {^{1}H} NMR ($CDCl_3$, 75 MHz): 15.1 (CH_3), 55.4 (CH_3), 58.8 (CH_3), 59.4 (CH_2), 68.2 (CH_2), 71.5 (CH_2), 94.5, 102.2, 114.4 (CH), 118.0 (CH), 119.1 (CH), 128.8 (CH), 130.0, 130.7 (CH), 131.2, 134.0 (CH), 135.3, 136.7, 138.1 (CH), 139.9, 152.2, 160.3. EI-MS (nature of the peak, relative intensity): 874.1 ([M], 100). $C_{47}H_{48}BIN_2O_6$ (Mr = 874.27) C, 64.54; H, 5.53; N, 3.20; Found C, 64.28; H, 5.29; N, 3.01.

8-(4-Trifluoromethyl-phenyl)-1,7-dimethyl-3,5-bis(4-methoxy-styryl-)-4,4-bis(2,5-dioxaoct-7-ynyl)-4-bora-3a,4a-diaza-s-indacene (2). The same procedure as for compound **1** was used starting from 8-(4-trifluoromethylphenyl)-1,7-dimethyl-3,5-bis(4-methoxy-styryl-)-4,4-difluoro-4-bora-3a,4a-diaza-s-indacene (0.1 g, 0.159 mmol) to afford compound **2** as blue powder (0.083 g, 64%). ^{1}H NMR ($CDCl_3$, 300 MHz): δ = 1.34 (s, 6H), 3.14–3.17 (m, 4H), 3.20 (s, 6H), 3.51–3.54 (m, 4H), 3.86 (s, 6H), 4.17 (s, 4H), 6.64 (s, 2H), 7.28 (ABsys, 8H, JAB = 8.6 Hz, ν0δ = 188.8 Hz), 7.62 (ABsys, 4H, JAB = 16.2 Hz, ν0δ = 288.7 Hz), 7.65 (ABsys, 4H, JAB = 7.9 Hz, ν0δ = 73.8 Hz); ^{13}C {^{1}H} NMR ($CDCl_3$, 75 MHz): 14.9, 55.3, 58.7, 59.4, 68.2, 71.5, 91.6, 114.5, 118.2, 118.9, 125.9 (q, J = 3.8 Hz), 128.8, 129.5, 129.9, 130.8, 131.1, 131.5, 134.3, 136.1, 139.6, 139.8, 152.3, 160.4. EI-MS (nature of the peak, relative intensity): 816.2 ([M], 100); $C_{48}H_{48}BF_3N_2O_6$ (Mr = 816.71) C, 70.59; H, 5.92; N, 3.43; Found C, 70.35; H, 5.78; N, 3.31.

Acknowledgements

We thank CNRS and UdS for partial financial support and Drs C. Andraud and O. Maury (ENS Lyon) for fruitful discussions.

Notes and references

1 J. W Lichtman and J.-A. Conchello, *Nature Methods*, 2005, **2**, 910–919; R. Yuste, *Nature Methods*, 2005, **2**, 902–904.
2 (*a*) P. J. Campagnola and L. M. Loew, *Nature Biotech.*, 2003, **21**, 1356–1360; F. Helmchen and W. Denk, *Nature Methods*, 2005, **2**, 932–940.
3 *Handbook of Cell-penetrating Peptides*, ed U. Langel, Second Emission, Taylor and Francis, CRC Press Book, 2006; F. Kielar, A. Congreve, G.-L. Law, E. J. New, D. Parker, K.-L. Wong, P. Castreno and J. de Mendoza, *Chem. Commun.*, 2008, 2435–2437.
4 S. Atilgan, Z. Ekmekci, A. L. Dogan, D. Guc and E. U Akkaya, *Chem. Commun.*, 2006, **42**, 4398–4400.
5 A. Loudet and K. Burgess, *Chem. Rev.*, 2007, **107**, 4891–4932; G. Ulrich, R. Ziessel and A. Harriman, *Angew. Chem., Int. Ed.*, 2008, **47**, 1184–1201.
6 R. Weissleder, *Nature Biotech.*, 2001, **19**, 316–317; R. Weissleder and V. Ntziachristos, *Nature Med.*, 2003, **9**, 123–128.
7 M. Pawlicki, H. A. Collins, R. G. Denning and H. L. Anderson, *Angew. Chem., Int. Ed.*, 2009, **48**, 3244–3266; O. Mongin, L. Porrès, M. Charlot, C. Katan and M. Blanchard-Desce, *Chem.–Eur. J.*, 2007, **13**, 1481–1498.
8 R. P. Haughland, H. C. Kang, *US. Patent* 1988, US4774339; N. Saki, T. Dinc and E. U. Akkaya, *Tetrahedron*, 2006, **62**, 2721–2725; R. Ziessel, G. Ulrich, A. Harriman, M. A. H. Alamiry, B. Stewart and P. Retailleau, *Chem.–Eur. J.*, 2009, **15**, 1359–1369.
9 C. Goze, G. Ulrich and R. Ziessel, *J. Org. Chem.*, 2007, **72**, 313–322.
10 T. M. Allen, P. Sapra, E. Moase, J. Moreira and D. Iden, *Journal of Liposome Research*, 2002, **12**, 1532–2394; Y. Gao, L. Chen, W. Gu, Y. Xi, L. Lin and Y. Li, *Molecular Pharmaceutics*, 2008, **5**, 1044–1054 and references therein.
11 R. Ziessel, L. Bonardi, P. Retailleau and G. Ulrich, *J. Org. Chem.*, 2006, **71**, 3093–3102; A. C. Benniston, G. Copley, K. J. Elliott, R. W. Harrington and W. Clegg, *Eur. J. Org. Chem.*, 2008, 2705–2713; S. Hisato, U. Yasuteru, K. Hirotatsu and N. Tetsuo, *J. Am. Chem. Soc.*, 2007, **129**, 5597–5604.
12 C. S. Sevier and C. A. Kaiser, *Nature Rev.*, 2002, **3**, 836–847.
13 Q. Zheng, G. Xu and P. N. Prasad, *Chem.–Eur. J.*, 2008, **14**, 5812–5819.
14 J. III Olmsted, *J. Phys. Chem.*, 1979, **83**, 2581–2584.
15 C. Xu, J. Guild, W. Webb and W. Denk, *Optics Letters*, 1995, **20**, 2372–2374.
16 M. Albota, D. Beljonne, J.-L. Brédas, J. E. Ehrlich, J.-Y. Fu, A. A. Heikal, S. E. Hess, T. Kogej, M. D. Levin, S. R. Marder, D. McCord-Maughon, J. W. Perry, H. Röckel, M. Rumi, G. Subramaniam, W. W. Webb, X.-L. Wu and C. Xu, *Science*, 1998, **281**, 1653–1656.
17 S. T. Hess, S. H. Huang, A. A. Heikal and W. W. Webb, *Biochemistry*, 2002, **41**, 697–705.
18 (*a*) S. Steenken and S. V. Jovanovic, *J. Am. Chem. Soc.*, 1997, **119**, 617–618; (*b*) D. H. Johnston, C.-C. Cheng, K. J. Campbell and H. H. Thorp, *Inorg. Chem.*, 1994, **33**, 6388–6390.
19 J. P. Rostron, G. Ulrich, P. Retailleau, A. Harriman and R. Ziessel, *New J. Chem.*, 2005, **29**, 1241–1244.
20 J. Azoulay, J. P. Clamme, J. L. Darlix, B. P. Roques and Y. Mély, *J. Mol. Biol.*, 2003, **326**, 691–700.
21 J. P. Clamme, J. Azoulay and Y. Mély, *Biophys. J.*, 2003, **84**, 1960–1968.
22 K. Brandner, A. Sambade, E. Boutant, P. Didier, Y. Mély, C. Ritzenthaler and M. Heinlein, *Plant Physiol.*, 2008, **147**, 611–23; J. V. Fritz, P. Didier, J. P. Clamme, E. Schaub, D. Muriaux, C. Cabanne, N. Morellet, S. Bouaziz, J. L. Darlix, Y. Mély and H. de Rocquigny, *Retrovirology*, 2008, **5**, 87–97.
23 A. Burghart, H. Kim, M. B. Wech, L. H. Thorensen, J. Reibenspies and K. Burgess, *J. Org. Chem.*, 1999, **64**, 7813–7819.

